

# The Effect of Hydrogen on the Surface Energy of Nickel

E. A. CLARK, R. YESKE, AND H. K. BIRNBAUM

The effect of hydrogen in solid solution in nickel on the surface and grain boundary free energies at 1573 K was determined using the zero creep technique. Effects of O and H adsorption on the surface free energies were considered and shown to have only small effects under the experimental conditions. The surface energy of pure nickel was determined to be about 2.34 J/m<sup>2</sup>. H concentrations of 300 at. ppm were shown to have no significant effect on the surface energy. Hydrogen had a somewhat greater effect on the grain boundary energy with  $\gamma_{\text{Ni}}^{GB}/\gamma_{\text{Ni-H}}^{GB} \approx 1.21$ . The implications of these results for hydrogen embrittlement mechanisms in Ni are discussed.

## 1. INTRODUCTION

WHILE hydrogen has demonstrably large effects on the mechanical properties of metals at both high and low temperatures, its detailed mechanistic role has not been clearly established in many systems. In many cases solute hydrogen or high hydrogen fugacity environments cause a transition in the fracture mode from ductile to brittle or a decrease in the amount of ductility prior to ductile fracture by microvoid coalescence. For systems in which hydrides do not form, these effects have often been interpreted<sup>1-6</sup> as due to decreases in the surface energy or the "cohesive energy" at the crack tip or to decreases of the interfacial energies at second phase particles<sup>7</sup> which are postulated to result from hydrogen in solid solution.

Hydrogen is known to strongly adsorb on clean metal surfaces<sup>8</sup> thereby reducing the surface energy. However, in the above phenomena the important question is whether hydrogen in solid solution decreases the "cohesive energy" and correspondingly the surface energy of metals leading to hydrogen embrittlement. In a recent review of the available experimental data Birnbaum<sup>1</sup> has concluded that little evidence in support of the postulated decrease in cohesive energy due to hydrogen exists. However, most of the data is available for Group V b hydride formers as these have relatively high hydrogen solubilities while the decohesion theories are generally applied to nonhydride formers having low hydrogen solubilities. In the present paper, a direct determination of the effect of hydrogen in solid solution on the surface energy of nickel is reported. Since nickel exhibits hydrogen embrittlement in the absence of hydride formation it is believed that this result has general applicability to nonhydride forming systems.

## 2. EXPERIMENTAL METHODS

The present experiments utilize the technique of zero creep which has been recently reviewed by Linford.<sup>9</sup> For the present purpose (assuming an elastically iso-

tropic solid, high temperatures and neglecting the variation of the surface energy with orientation) it can be shown that the surface energy free  $\gamma$ , *i.e.* the partial Helmholtz free energy with respect to area, is numerically equal to the surface tension which is the magnitude of the diagonal terms of the two-dimensional surface stress tensor. The surface free energy can be determined at elevated temperatures by equilibrating the surface tension with the gravitational force acting on a weight supported by a thin wire or sheet specimen. At a weight  $W_0$  such that the creep rate of the specimen is zero, the force balance can be written<sup>9</sup> for a bamboo grain structure as follows;

$$W_0 = \pi r \gamma - \frac{n}{l} \pi r^2 \gamma^{GB} \quad [1]$$

where  $r$  is the wire radius,  $n$  is the number of grain boundaries in the gage length  $l$ , and  $\gamma^{GB}$  is the grain boundary energy. The grain boundary energy must be determined independently by measuring the dihedral angle,  $\theta_D$  of the groove formed at the intersection of the grain boundaries with the surface and applying the surface tension balance equation,<sup>9,10</sup>

$$\gamma^{GB}/\gamma = 2 \cos(\theta_D/2). \quad [2]$$

Application of Eqs. [1] and [2] requires careful consideration of impurity adsorption at the surfaces as this can decrease the measured energies. The effect of an adsorbed ideal diatomic gas on the surface energy, is expressed by the Gibbs adsorption isotherm,<sup>9</sup>

$$\Gamma = - \frac{2}{kT} \left( \frac{\partial \gamma}{\partial \ln p_i} \right)_{T,p}. \quad [3]$$

In this relation,  $\Gamma$  is the surface excess coverage, or the number of atoms absorbed per unit area,  $k$  is Boltzmann's constant,  $T$  is the absolute temperature,  $p_i$  is the partial pressure of the diatomic gas, and  $p$  is the total pressure. This relation must be considered in relation to the Langmuir isotherm<sup>11</sup>

$$p_i = \frac{\theta}{1 - \theta} \exp \left( \frac{\Delta H - T \Delta S}{RT} \right) \quad [4]$$

where  $\theta$  is the fraction of surface sites occupied by adsorbed atoms and  $\Delta H$  and  $\Delta S$  are the enthalpy and

E. A. CLARK is Research Assistant and H. K. BIRNBAUM is Professor at the University of Illinois, Department of Metallurgy and Mining Engineering. R. YESKE is Research Scientist, Westinghouse Research and Development Center, Pittsburgh, PA.

Manuscript submitted February 4, 1980.

entropy of adsorption which are assumed to be constant over the range of coverages considered.

The variation of surface energy with surface coverage may be obtained by combining Eqs. [3] and [4] to yield

$$\gamma^0 - \gamma = -\frac{kTn_s}{2} \ln(1 - \theta) \quad [5]$$

where  $\gamma^0$  is the surface energy of the clean surface,  $\gamma$  is the surface energy with a coverage  $\theta$  and  $n_s$  is the number of surface sites/unit area. Thus measurement of  $\gamma$  and  $\theta$  should allow an estimate of  $\gamma^0$  under the assumptions which lead to the Langmuir isotherm, Eq. [4].

The zero creep measurements were carried out in the apparatus shown schematically in Fig. 1. The specimen chamber was machined entirely of nickel and the nominally 130  $\mu\text{m}$  wire specimens were spot welded to the cap and therefore were entirely surrounded by nickel. The nickel chamber was heated inductively. A feedback temperature controller was used, allowing control to about  $\pm 3$  K over 24 h. One tungsten-25 pct rhenium/tungsten-3 pct rhenium thermocouple was used to control and the other to monitor the temperature.

The creep measurements were carried out either in purified argon atmospheres at a pressure of 120 kPa or in a 50 kPa argon/70 kPa hydrogen mixture. The latter was used to reduce the evaporation of nickel which occurred when pure hydrogen atmospheres were used. The argon used was ultrahigh purity (99.9995 pct) and was further purified by passing the gas over titanium chips at 773 K. The hydrogen used was also ultrahigh purity (99.9995 pct). Further purification of the gas occurred by the gettering action of the nickel evaporated on the cold quartz walls of the vacuum chamber adjacent to the nickel chamber. The nickel surfaces remained clean, showing no evidence of oxidation even when examined at high magnification; under all the atmosphere conditions used.

The specimens used were 130  $\mu\text{m}$  diam high purity nickel wires having the analyses given in Tables I(a) and

(b). Gage marks were cut with razor blades in a special jig, and weights were made of the same wire, coiled and melted on a charcoal block. Each run used six samples with varying weights.

A precreep vacuum anneal was performed at 1023 K before every run until the pressure fell to below  $3 \times 10^{-4}$  Pa. The vacuum system was then backfilled to a total pressure of 120 kPa and 24 h creep tests were performed at 1573 K. The gage length was measured after each test with a travelling microscope to a precision of  $\pm 5.0 \mu\text{m}$ .

After several tests in a given atmosphere, the wires were carefully removed from the cap and the number of grain boundaries was counted for each specimen's gage length using an optical metallograph with a magnification of about 50 diameters. The mass of the bottom half of the wires plus the attached weight was determined to  $\pm 0.1$  mg. The specimen diameter and dihedral angles of the intersection of grain boundaries with the surface were measured by scanning electron microscopy.

### 3. RESULTS

The steady state strain rates were calculated for each specimen from the measured specimen strain vs time and these strain rates were used to determine weight  $W_0$  for zero creep rate. The specimen weights were chosen to bracket  $W_0$  so both positive and negative strain rates were observed. All data analyses used linear regression methods. The experimental values of  $W_0$  as well as the average number of grains per unit length  $n$ , the average grain boundary dihedral angle  $\theta_D$  and the average wire radius  $r$  are shown in Table II.

The surface energies  $\gamma$  and grain boundary energies  $\gamma^{GB}$  calculated using Eqs. [1] and [2] are also given in Table II. It is seen that the most probable value of  $\gamma$  in

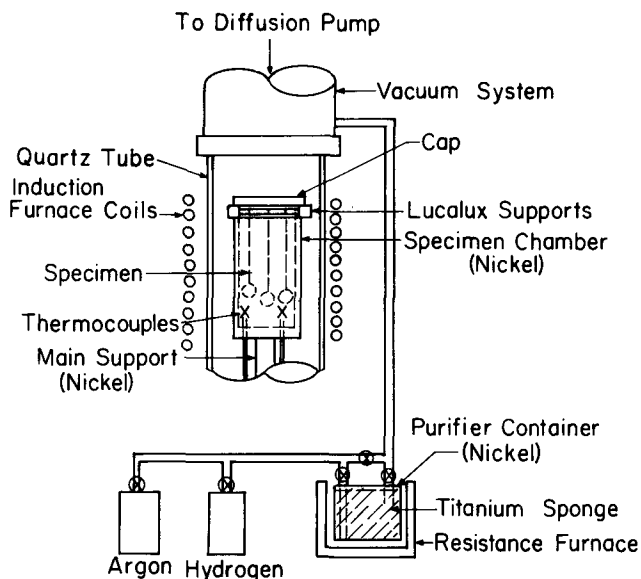


Fig. 1—Schematic diagram of the experimental apparatus.

Table I(a). Mass Spectrographic Analysis of Nickel Wire

Element	Concentration (appm)	Element	Concentration (appm)
Pb	2	Cr	0.8
Ta	0.8	V	0.08
Hf	0.2	Ti	0.2
Sn	9	Ca	4
Nb	0.9		
Zr	0.1		
As	0.8	S	20
Zn	0.5		
Cu	1	Si	20
Co	0.8	Al	0.8
Fe	7	Mg	30
Mn	0.2	Na	7

Table I(b). Vacuum Fusion Analysis of Nickel Wire\*

Element	Concentration, appm
H	1298
C	295
O	531

\* Analysis taken prior to anneals.

**Table II. Experimental Results**

Hydrogen/Argon		
Quantity	No. of Observations	Value
$W_o$	—	$44.6 \times 10^{-5} \text{ N} \pm 5.8 \times 10^{-5}$
$\bar{n}$	6*	$2.7 \times 10^3 \text{ m}^{-1} \pm 0.4 \times 10^3$
$\theta_D$	30	$167^\circ \pm 2^\circ$
$r$	6	$6.68 \times 10^{-5} \text{ m} \pm 0.05 \times 10^{-5}$
$\gamma$	—	$2.21 \text{ J/m}^2 \pm 25\%$
$\gamma^{GB}$	—	$0.47 \text{ J/m}^2$
$\gamma^{GB}/\gamma$	—	0.21
Argon		
Quantity	No. of Observations	Value
$W_o$	—	$33.9 \times 10^{-5} \text{ N} \pm 7.9 \times 10^{-5}$
$\bar{n}$	6*	$3.3 \times 10^3 \text{ m}^{-1} \pm 0.5 \times 10^3$
$\theta_D$	23	$162^\circ \pm 3^\circ$
$r$	6	$6.51 \times 10^{-5} \text{ m} \pm 0.04 \times 10^{-5}$
$\gamma$	—	$1.78 \text{ J/m}^2 \pm 14\%$
$\gamma^{GB}$	—	$0.57 \text{ J/m}^2$
$\gamma^{GB}/\gamma$	—	0.32

\* The number of grain boundaries in the gage length of each of six specimens was counted and the resulting number of boundaries per unit length was averaged.

the hydrogen/argon atmosphere is larger than  $\gamma$  in the argon atmosphere. This difference is within the estimated error limits discussed below, however. The grain boundary energies  $\gamma^{GB}$  in the hydrogen/argon atmosphere are less than those for the argon atmosphere, with the difference again being within the estimated error.

The given intervals for  $n$ ,  $\theta_D$  and  $r$  in Table II are for one standard deviation. The interval for  $W_o$  is found for a confidence of 0.50 using the analysis of probable errors of least-square fitting presented by Bowker and Lieberman<sup>12</sup> and the error in  $\gamma$  is calculated from an analysis of the propagation of errors.<sup>13</sup> The largest source of error in  $\gamma$  represents the error in determining  $W_o$ .

#### 4. DISCUSSION

The main result of these experiments is that the surface energy of the Ni-H solid solution (measured in H-Ar atmospheres) is equal to or somewhat greater than that of pure Ni (measured in the Ar atmospheres). Consideration of this result requires a discussion of the state of the surfaces in both cases since adsorption of a second species always leads to a decrease of the surface energy (Eq. [3]) relative to a clean surface. It will be shown that the surface excess coverage of hydrogen and oxygen in the H-Ar atmospheres was very low and therefore the measured values are characteristic of the Ni-H solid solution. In the Ar atmosphere significant surface coverage of oxygen occurred. The value of the true surface energy of Ni will be estimated and shown to be about equal to that of the Ni-H alloy.

The extent of H coverage of the Ni surface,  $\theta_H$ , in the Ar-H atmospheres can be estimated from Eq. [4] using the heat of adsorption of H on Ni which was determined by Christmann *et al*<sup>8</sup> to be  $-96 \text{ kJ/mol}$  ( $-23 \text{ kcal/mol}$ ). A reasonable estimate for the entropy of adsorption of a diatomic gas on a metal surface is given following Trapnell<sup>14</sup> to be about  $-126 \text{ J/mol K}$  ( $-30$

$\text{kcal/mol K}$ ). For the hydrogen partial pressure of 70 kPa this gives a coverage of  $\theta_H = 2 \times 10^{-4}$  at 1573 K. Since the heat of the adsorption of H on a grain boundary is expected to be less than at a free surface, this coverage,  $\theta_H = 2 \times 10^{-4}$  is an upper bound for the H at grain boundaries at the 1573 K measuring temperature.

The oxygen coverage,  $\theta_o$ , in the Ar-H atmospheres cannot be calculated directly since the oxygen and  $\text{H}_2\text{O}$  partial pressures were not determined. This value can however be estimated by considering the equilibrium between Ni, NiO, adsorbed O and the gas phase components. The standard state Gibbs free energy for the reaction



is  $\Delta G_{1573}^0 = 71 \text{ kJ}^{15}$  leading to

$$(p_{\text{H}_2\text{O}}/p_{\text{H}_2}) \geq 233$$

for formation of NiO. The gas atmosphere contained an initial total impurity content of the order of  $5 \times 10^{-6}$  (corresponding to  $(p_{\text{H}_2\text{O}} + p_{\text{O}_2})/p_{\text{H}_2} \leq 5 \times 10^{-6}$ ). The actual atmosphere in contact with the specimens is expected to be appreciably purer than this as the specimens were completely enclosed in a Ni container and the evaporation of Ni onto the cold vacuum chamber walls served to continuously getter the atmosphere. Thus no NiO is expected to form and none was observed on microscopic examination of the specimens after the measurements. Adsorbed oxygen,  $\text{O}_{\text{ads}}$ , is also reduced by the  $\text{H}_2$  atmosphere at 1573 K according to the reaction



which has a Gibbs free energy  $\Delta G^0 = -31.5 \text{ KJ}$ . The activity of the adsorbed oxygen is therefore given by

$$a_{\text{O}_{\text{ads}}} = 0.088 p_{\text{H}_2\text{O}}/p_{\text{H}_2}$$

and for the  $p_{\text{H}_2\text{O}}/p_{\text{H}_2}$  estimated above the

$$a_{\text{O}_{\text{ads}}} < 4 \times 10^{-7}$$

corresponding to a clean nickel surface.

Hydrogen solubility in nickel at 1573 K and 70 kPa hydrogen partial pressure can be estimated to be 300 atomic ppm using Robertson's<sup>16</sup> data. Thus we conclude that the value of  $2.21 \text{ J/m}^2$  obtained for the H-Ar measurements at 1573 K corresponds to the surface energy of a Ni-300 appm H solid solution having "clean" surfaces with low H and O coverages.

Despite the absence of a reducing atmosphere, the Ar gas was sufficiently pure to prevent any oxidation of the nickel specimens. Since the dissociation pressure of NiO at 1573 K is 0.1 Pa this sets an upper limit to the oxygen partial pressure which is consistent with the upper limit previously estimated from the gas purity. The oxygen surface coverage  $\theta_o$  can be estimated (Eq. [4]) for a reasonable range of oxygen partial pressures below the upper limit and the measured surface energy can be corrected for the effects of this adsorption (Eq. [5]). These results are given in Table III along with the estimated concentrations of O in solid solution.\* The

\* The concentration of oxygen in solid solution in equilibrium with the gas phase was estimated using values for the solvus concentration in equilibrium with NiO, the dissociation pressure of NiO and the assumption of a regular solid solution.

effect of adsorbed oxygen on the surface energy is significant but the corrected clean surface energy values for Ni are not significantly different than that measured for the Ni-300 at. ppm alloy.

Values of the surface energy and grain boundary energy values obtained in the present study are compared to those obtained for nickel in previous investigations in Table IV. While Stickle *et al.*<sup>17</sup> attempted to control the oxygen partial pressures using a solid zirconia electrolyte their data exhibited a large scatter as shown in Table IV. Their value for the surface energy obtained at the lowest  $p_{O_2}$  is in good agreement with our corrected value as are the values obtained by Roth<sup>18</sup> and Murr *et al.*<sup>21</sup> Most of the literature surface energy values are lower than the present values as might be expected from oxygen adsorption effects.

The ratio of the nickel surface free energy,  $\gamma_{Ni}^{corr}$  to that of the Ni-300 at. ppm H surface free energy,  $\gamma_{Ni-H}$  is  $\gamma_{Ni}/\gamma_{Ni-H} \leq 1.06$  which shows no significant decrease of the surface energy on alloying with hydrogen. These values, obtained at 1573 K can be corrected for lower temperatures using surface entropies. Since values of the surface entropies are of the order of  $10^{-3} \text{ J/m}^2/\text{K}$  the 1573 K surface free energy values are increased by about  $1.25 \text{ J/m}^2$  at 300 K. Furthermore, examination of the experimental data for surface energies measured at various temperatures suggests that the effect of hydrogen on the surface entropy is not significant, particularly in view of the minor effects of hydrogen on the surface free energy. Thus the ratio  $\gamma_{Ni}/\gamma_{Ni-H}$  is expected to be relatively insensitive to temperature at constant  $\theta_H$  on the surface and on the grain boundaries.

Hydrogen effects on the grain boundary energy of nickel appear to be somewhat larger than for the

surface energy. The ratio  $\gamma_{Ni}^{GB}/\gamma_{Ni-H}^{GB}$  is 1.21 suggesting that 300 at. ppm of H in solid solution decreases the grain boundary energy by about 17 pct. This conclusion is made somewhat uncertain by the lack of knowledge of the segregation of other solutes at the grain boundaries; a possibility which may account for the variability of  $\gamma^{GB}$  between different investigations as shown in Table IV.

The question of whether H has a significant effect on the lattice energies of metals has been discussed extensively in the literature on hydrogen embrittlement.<sup>1-7</sup> Recently Oriani<sup>24</sup> and Seah<sup>25,26</sup> have related the maximum stress  $\sigma_m$  obtained on uniformly separating a crystal across an atomic plane or boundary to the stress for fracture and have suggested that decreases in  $\sigma_m$  due to H in the lattice or adsorbed on the boundary can account for hydrogen embrittlement. Since nickel exhibits both transgranular and intergranular hydrogen embrittlement<sup>27</sup> the present results can be usefully discussed in the context of the "decohesion" mechanisms of hydrogen embrittlement. In the following discussion we shall discuss fracture in terms of the surface energy terms despite the actual significance of plastic work terms. In order that a decohesion type theory be applicable, these surface energy terms must dominate; perhaps as a result of a scaling of the plastic work with the true surface energy as suggested by Vitek and McMahon.<sup>28</sup>

The thermodynamics of fracture have been recently discussed by Rice<sup>4</sup> and Hirth<sup>29</sup> who showed that

$$\phi = 2\gamma_A^s - \gamma_A^b - \int_{\mu_1^*}^{\mu_2^*} (2\Gamma_2^s - \Gamma_2^b) d\mu_2 \quad [8]$$

where  $\phi$  is the isothermal work of fracture per unit area,

Table III. Summary of Measured and Calculated Results

Atmosphere (kPa)	$p_{O_2}^*$ (Pa)	$C_H$ (at. fract.)	$C_o^*$ (at. fract.)	$\theta_H^*$	$\theta_o^*$	$\gamma_{meas.}$ (J/m <sup>2</sup> )	$\gamma_{corr.}$ (J/m <sup>2</sup> )
50 Ar/70H <sub>2</sub>	<0.1	$3 \times 10^{-4}$	$<4 \times 10^{-4}$	$<2 \times 10^{-4}$	$<4 \times 10^{-7}$	2.21	2.21
120 Ar	0.1	0	$4 \times 10^{-4}$	0	0.998	1.78	2.34
	$10^{-3}$	0	$4 \times 10^{-5}$	0	0.86	1.78	1.95
	$10^{-4}$	0	$1 \times 10^{-5}$	0	0.38	1.78	1.82

\* Estimated values; see text.

Table IV. Summary of Investigations of Nickel Surface Energy

Reference	Temperature, K	Atmosphere	$\gamma$ (J/m <sup>2</sup> )	Plane	$\gamma^{GB}$ (J/m <sup>2</sup> )	$\gamma^{GB}/\gamma$
Present Work	1573	Ar	1.78		0.57	0.32
Present Work	1573	Ar (Corrected)	<2.34	—	—	—
Present Work	1573	H <sub>2</sub> /Ar	2.21		0.47	0.21
18	1573	$10^{-6}$ Pa O <sub>2</sub>	2.01		—	—
18	1573	$10^{-7}$ Pa O <sub>2</sub>	1.29		—	—
18	1573	$10^{-13}$ Pa O <sub>2</sub>	2.19		—	—
19	1643	He	2.49		0.93	0.37
20	1492	$10^{-6}$ Pa	1.82	(100)	—	—
20	1492	$10^{-6}$ Pa	1.90	(110)	—	—
21	1673	$10^{-2}$ Pa	1.94		—	—
22	1333	He	2.28		0.87	0.38
23	1523	Ar	1.85		0.74	0.40
23	1726	Ar	1.73		0.69	0.40
24	1573	"Vacuum"	—		—	0.26

$\gamma_A^s$  and  $\gamma_A^b$  are the surface free energies of the external and grain boundaries respectively,  $\Gamma_2^s$  and  $\Gamma_2^b$  are surface and grain boundary excess compositions of the solute (H) denoted as component 2, and  $\mu_2$  is the chemical potential of the solute. Equation 8 describes intergranular fracture along a grain boundary while for transgranular fracture the terms pertaining to the grain boundary would be identically zero.

Equation 8 can be used to describe fracture at a constant solute chemical potential such as would be set by equilibration with a constant  $H_2$  gas pressure. In this case the thermodynamic state  $A$  is the pure solvent and the state  $B$  is the alloy state in equilibrium with the external gas pressure. For this situation the pure solvent surface free energy terms ( $2\gamma_A^s - \gamma_A^b$ ) are modified by the work of solute adsorption on the surfaces given by the integral terms. Under conditions where equilibration of the solute cannot occur, Eq. [8] can also describe the fracture energy with a redefinition of terms. Under these conditions the thermodynamic state  $A$  is that in equilibrium with the grain boundary or atomic fracture plane prior to fracture while  $B$  is that which would be in equilibrium with the surfaces after fracture. The alloy surface energy terms ( $2\gamma_A^s - \gamma_A^b$ ) are again modified by the solute adsorption terms given by the integral.

The general result obtained in the present experiment is that  $\gamma_{Ni}^s \approx \gamma_{Ni-H}^s$  leading to the results for transgranular fracture that

$$\phi_{Ni-H} = \phi_{Ni} - 2 \int_{\mu_{Ni}^s}^{\mu_{Ni-H}^s} \Gamma_H^s d\mu_H \quad [9]$$

for fracture under equilibrium conditions and

$$\phi_{Ni-H} = \phi_{Ni} - 2 \int_{\mu_{Ni-H,A}^s}^{\mu_{Ni-H,B}^s} \Gamma_H^s d\mu_H \quad [10]$$

for fracture under conditions where the H is immobile. The fracture work  $\phi_{Ni} = 2\gamma_{Ni}^s - \gamma_{Ni}^b$ . In the case of intergranular fracture the results that  $\gamma_{Ni}^s \approx \gamma_{Ni-H}^s$  and  $\gamma_{Ni}^b \approx 1.21 \gamma_{Ni-H}^b$  lead to

$$\phi_{Ni-H} = \phi_{Ni} - \int_{\mu_{Ni}^s}^{\mu_{Ni-H}^s} (2\Gamma_H^s - \Gamma_H^b) d\mu_H \quad [11]$$

for fracture under equilibrium conditions and

$$\phi_{Ni-H} = 2\gamma_{Ni} - 0.83\gamma_{Ni} - \int_{\mu_{Ni-H,A}^s}^{\mu_{Ni-H,B}^s} (2\Gamma_H^s - \Gamma_H^b) d\mu_H \quad [12]$$

for fracture under conditions where the H is immobile.

As shown in Eqs. [9] to [11] the reduction in the work for fracture of the Ni-H alloy is due to the work of H adsorption on the surfaces rather than due to a change in atomic bonding across atomic planes or grain boundaries in the solid solution in the absence of H surface segregation. This conclusion is only approximately true for transgranular fracture under conditions where the reduction of grain boundary energy by hydrogen actually increases the work for fracture (Eq. [12]). It follows that hydrogen effects on fracture (under conditions where the fracture energy is determined by surface energy terms) are a consequence of the influence of local hydrogen concentrations on bonding across interfaces rather than a more global influence of

distributed hydrogen concentrations on the atomic bond strength in the volume of a crystal.

## 5. CONCLUSIONS

Equilibrium measurements of the surface free energy of Ni and Ni containing 300 at. ppm H were made at 1573 K. Analysis of the results indicate that:

- the surface free energy of pure Ni is about 2.34 J/m<sup>2</sup>. (This value is an upper limit).
- the surface free energy of Ni + 300 at. ppm H is 2.21 J/m<sup>2</sup>,
- no significant reduction of the surface free energy results from hydrogen in solid solution at the 300 at. ppm H level,
- a decrease of the grain boundary energy due to hydrogen in solid solution was observed;

$$\gamma_{Ni}^{GB} / \gamma_{Ni-H}^{GB} \approx 1.21.$$

Consideration of the thermodynamics of crack extension, combined with the above observations leads to the conclusion that hydrogen solutes can decrease the work for intergranular or transgranular fracture due to adsorption effects at the surfaces and not by significantly altering the lattice potential between the solvent atoms in the solid solution in the absence of H segregation to surfaces.

This work was supported by the National Science Foundation Grant DMR 77-09808.

## REFERENCES

- H. K. Birnbaum: *Environment-Sensitive Fracture of Engineering Materials*, Z. A. Foroulis, ed., p. 326, The Metallurgical Society of AIME, Warrendale, PA, 1979.
- N. J. Petch: *Philos. Mag.*, 1956, Ser. 8, vol. 1, p. 331.
- R. A. Oriani and P. H. Josephic: *Acta Metall.*, 1974, vol. 22, p. 1065.
- J. R. Rice: *Effect of Hydrogen on Behavior of Materials*, A. W. Thompson and I. M. Bernstein, eds., p. 455, American Institute of Mining, Metallurgical and Petroleum Engineers, New York, N.Y., 1976.
- R. A. Oriani: *Ber. Bunsenges. Phys. Chem.*, 1972, vol. 76, p. 848.
- J. P. Hirth and H. H. Johnson: *Corrosion*, 1976, vol. 32, p. 3.
- A. W. Thompson: *Effect of Hydrogen on Behavior of Materials*, A. W. Thompson and I. M. Bernstein, eds., p. 467, American Institute of Mining, Metallurgical and Petroleum Engineers, New York, 1976.
- K. Christmann, O. Schober, E. Ertl, and M. Newmann: *J. chem. Phys.*, 1974, vol. 60, p. 4528.
- R. G. Linford: *Solid State Surface Science*, Mino Green, ed., vol. 2, p. 1, Marcel Dekker, New York, 1973.
- H. Udin: *Metal Interfaces*, p. 114, American Society for Metals, Cleveland, OH, 1952.
- K. Denbeigh: *The Principles of Chemical Equilibrium*, 3rd ed., p. 436-38, Cambridge University Press, London, 1971.
- A. H. Bowker and G. J. Lieberman: *Engineering Statistics*, 2nd ed., pp. 336-37 and 340-42, Prentice-Hall, Englewood Cliffs, NJ, 1972.
- Y. Beers: *Introduction to the Theory of Error*, 2nd ed., pp. 26-29, Addison-Wesley, Reading, MA, 1957.
- B. M. W. Trapnell: *Chemisorption*, p. 212, Academic Press, New York, 1955.
- T. Rosenqvist: *Principles of Extractive Metallurgy*, p. 516, McGraw-Hill, New York, 1974.
- W. M. Robertson: *Z. Metallkd.*, 1973, vol. 64, p. 436.
- D. R. Stickle, J. P. Hirth, G. Meyrick, and R. Speiser: *Met. Trans. A*, 1976, vol. 7A, p. 71.
- T. A. Roth: *Mater. Sci. Eng.*, 1975, vol. 18, p. 183.
- P. S. Maiya and J. M. Blakely: *J. Appl. Phys.*, 1967, vol. 38, p. 698.

20. R. M. Digilov, S. N. Zadumkin, V. K. Kумыков, and Kh. B. Khokonov: *Phys. Met. Metall.*, 1976, vol. 41, p. 68.
21. L. E. Murr, O. T. Inal, and G. I. Wong: *Electron Microscopy and the Structure of Metals*, G. Thomas, ed., p. 471, University of California Press, Berkeley, CA, 1972.
22. E. R. Hayward and A. P. Greenough: *J. Inst. Met.*, 1959, vol. 88, p. 217.
23. T. M. Williams and P. Barrand: *J. Inst. Met.*, 1965, vol. 93, p. 447.
24. R. A. Oriani: *Ber. Bunsenges. Phys. Chem.*, 1972, vol. 76, p. 848.
25. M. P. Seah: *Surf. Sci.*, 1975, vol. 53, p. 168.
26. M. P. Seah: *Proc. R. Soc. London*, 1976, vol. A349, p. 539.
27. T. Matsumoto and H. K. Birnbaum: *Trans. Jpn. Inst. Met.*, 1980, vol. 21, p. 493.
28. C. J. McMahon, Jr. and V. Vitek: *Acta Metall.*, 1979, vol. 27, p. 507.
29. J. P. Hirth: *Phil. Trans. R. Soc. London*, 1980, vol. A295, p. 139.